

Integrated Analysis of lncRNA, miRNA and mRNA Reveals Novel Insights into the Fertility Regulation of Large White Sows

Huiyan Hu

Agricultural University of Hebei <https://orcid.org/0000-0002-8138-7336>

Qing Jia (✉ auhjq@163.com)

Jianzhong Xi

Hebei Agriculture University

Bo Zhou

Hebei Agriculture University

Zhiqiang Li

Hebei Agriculture University

Research article

Keywords: pigs, fertility, ovary, follicular and luteal phases, competing endogenous RNAs, regulation networks

Posted Date: September 30th, 2019

DOI: <https://doi.org/10.21203/rs.2.15328/v1>

License:  This work is licensed under a Creative Commons Attribution 4.0 International License.

[Read Full License](#)

Version of Record: A version of this preprint was published on September 14th, 2020. See the published version at <https://doi.org/10.1186/s12864-020-07055-2>.

Abstract

Background: Improving sow fertility is extremely important as it can lead to increased reproductive efficiency and thus profitability for swine producers. There are considerable differences in fertility rates among individual animals, but the underlying molecular mechanisms remain unclear. In this study, by using different types of RNA libraries, we investigated the complete transcriptome of ovarian tissue during the luteal (L) and follicular phases (F) of the estrous cycle in Large White pigs with high (H) and low fecundity (L), and performed a comprehensive analysis of long noncoding RNAs (lncRNAs), mRNAs and micro RNAs (miRNAs) from 16 samples by combining RNA sequencing (RNA-seq) with bioinformatics.

Results: In total, 24,447 lncRNAs, 27,370 mRNAs, and 216 known miRNAs were identified in ovarian tissues. The genomic features of lncRNAs, such as length distribution and number of exons, were further analyzed. We selected a threshold of $P < 0.05$ and $|log_2(\text{fold change})| \geq 1$ to obtain the differentially expressed lncRNAs, miRNAs and mRNAs by pairwise comparison (LH vs. LL, FH vs. FL). Bioinformatics analysis of these differentially expressed RNAs revealed multiple significantly enriched pathways ($P < 0.05$) that were closely involved in the reproductive process, such as ovarian steroidogenesis, lysosome, steroid biosynthesis, and the estrogen and GnRH signaling pathways. Moreover, bioinformatics screening of differentially expressed miRNAs that share common miRNA response elements (MREs) with lncRNAs and their downstream mRNA targets were performed. Finally, we constructed lncRNA–miRNA–mRNA regulation networks. The key genes in these networks were verified by Reverse Transcription Real-time Quantitative PCR (RT-qPCR), which were consistent with the results from RNA-Seq data.

Conclusions: These results provide further insights into the fertility of pigs and can contribute to further experimental investigation of the functions of these genes.

Background

Sow fertility is one of the most important economic parameters in the swine industry, and therefore improving reproduction rate can significantly increase the profitability for swine producers. Candidate genes and quantitative trait loci (QTL) associated with reproductive traits, such as total number (of piglets) born (TNB), have been identified in genome-wide association studies (GWAS) in the past [1–6]. Thus far, 377 quantitative trait loci (QTL) for reproductive traits were detected, of which 159 and 129 QTLs for TNB and number born alive (NBA) have already been identified, respectively [7]. Although GWAS results provide important information regarding specific reproductive traits, revealing the complex regulatory mechanism of reproductive performance is still a challenging task. Therefore, the underlying mechanisms of fertility differences in sows are the subject of constant research.

The mammalian genome encodes a high percentage of noncoding transcripts [8]. Two major subsets of noncoding RNAs (ncRNAs) have been identified by high-throughput sequencing: long noncoding RNAs (lncRNAs) and microRNAs (miRNAs) [9]. lncRNAs are a group of regulatory RNAs that are longer than 200

nucleotides and were recently identified in various tissues [10–12]. On the other hand, miRNAs are an abundant class of short (18–24 nucleotides) and highly conserved sequences of endogenous RNAs, which have been extensively studied in many animals [13]. Previous studies have prospectively confirmed that ncRNAs (miRNAs and lncRNAs) were considered as crucial players in both humans and animals, and affect various biological functions [12, 14–16]. According to the hypothesis of competing endogenous RNAs (ceRNAs) [17], there is substantial evidence supporting that lncRNAs, acting as ceRNAs, contribute to the regulation of cardiac fibrosis [18], muscle differentiation [19] and tumorigenesis [20, 21].

The ovary is the most important reproductive organ of sows and is responsible for synthesizing and secreting hormones, which are essential for the maintenance of the normal reproductive cycles and hormone levels. Ovarian folliculogenesis, ovulation and formation and regression of the corpus luteum occur in the ovary, which repeatedly take place over the reproductive life [22] and regulate reproduction in mammals [23]. Previous reports have shown that miRNAs are involved in ovarian processes [24] and regulate fertility [25, 26]. In addition, lncRNAs represent another category of functional RNA molecules. A recent study demonstrated that lncRNAs also play a significant role in the regulation of sheep fertility [27]. While several articles have focused on the lncRNAs expression profile of pig ovarian tissues [28, 29], none of these studies have interpreted regulatory networks for fertility.

In order to improve our understanding of differences in reproductive performance, we constructed and sequenced two different types of cDNA sequence libraries (16 RNA libraries and 16 small RNA cDNA libraries) from ovarian tissue during the follicular and luteal phases of the estrous cycle in Large White pigs with extreme phenotypes (high and low fertility). We aimed to identify potential regulators (lncRNAs and miRNAs) of fecundity in pigs. Importantly, data in this study were integrated in order to reveal novel insights into molecular mechanisms between the high and low fertility in pigs.

Results

Characterization of the ovary transcriptome and identification of mRNA and lncRNAs

To identify key differences associated with reproductive efficiency in sows with extreme phenotypes, we constructed 16 cDNA libraries from ovarian tissues during the follicular and luteal phases of the estrous cycle. A total of 1,509,728,794 raw reads were generated from 16 porcine ovary samples. After removing adapter sequences and low-quality sequences, 1,500,044,340 clean reads were retained and used for further analysis. In each sample, the percentage of clean reads ranged from 99.20% to 99.52% (Additional file 2: Table S2–1). In addition, most clean reads were aligned to the reference genome (Sscrofa10.2), accounting for 81.49% to 84.48% (Table S2–2). A total of 1,122,470 transcripts were assembled by Cuffmerge and Scripture [30]. According to the characteristics of lncRNAs, we used four tools (CPC, CNCI, CPAT and PFAM) to discard potential coding transcripts. In the end, 24,447 lncRNA transcripts were identified (Additional file 3: Table S3). These included 6,392 anti-sense lncRNAs (26.15%) and 18,055 intergenic lncRNAs (73.85%) (Table S3). In addition, 27,370 mRNAs were identified by mapping Illumina RNA-seqreads (Additional file 4: Table S4).

microRNA sequencing and identification

Sequencing data from 16 ovarian small RNA was generated on Illumina HiSeq and provided a total of 433,792,963 raw reads. After filtering out the low-quality sequences, including adaptor dimmers and less than 18 nt, 363,273,750 clean reads were ultimately achieved. The percentage of clean reads ranged from 74.75% to 88.31% in each small RNA library (Additional file 5: Table S5–1). The length distribution of clean reads showed that most of the reads were 20–24 nt, and 22 nt was the most abundant length identified. Such reads accounted for 36.30% of the total sequences (Additional file 5: Table S5–2). In total, 216 known miRNAs (Additional file 6: Table S6–1) and 1,724 novel miRNAs (Additional file 6: Table S6–2) were identified, while 198 known miRNAs were expressed in all four groups (Fig. 1).

Genomic features and expression patterns of lncRNAs

Overall, 24,447 lncRNAs and 27,370 mRNAs were detected in the ovaries of all 16 individual sows. In order to examine the differences in features between lncRNAs and mRNAs in ovarian tissues, their lengths were compared. The average length of lncRNAs was 2,955 bp, which was longer than that of the mRNAs (Fig. 2A). We also observed that the number of exons of lncRNAs was lower than that of the mRNAs, which tend to contain 2.3 exons (Fig. 2B). The ORFs of the lncRNAs were shorter than those of the mRNAs (Fig. 2C). Lastly, their expression levels were also compared (Fig. 3); In general, lncRNAs had lower expression levels.

lncRNAs can act in cis or trans to positively or negatively regulate gene expression; however, cis-acting lncRNAs are restricted to the chromosome from which they are transcribed. To further explore the relationship between lncRNAs and their neighboring coding genes in ovarian tissues, we searched for neighboring protein-coding genes (<10k) of all the identified lncRNAs and analyzed gene pairs formed by lncRNAs and their neighboring genes. We identified 4,044 protein-coding genes: coding gene pairs (873 in divergent) and 1,664 lncRNA: coding gene pairs (195 in divergent) (Fig. 4). We observed that the expression pattern of lncRNAs with their neighboring gene pairs (average Pearson correlation: 0.20) was similar to the coding gene pairs (average Pearson correlation: 0.28) and exhibited a significantly higher correlation than random coding gene pairs (average Pearson correlation: 0.041, $P < 0.01$) (Fig. 5A). We observed that there was a relatively low correlation between divergent lncRNAs: coding gene pairs (average correlation: 0.19) than divergent coding gene pairs (average Pearson correlation: 0.30, $P < 0.05$), and a higher correlation compared with random coding gene pairs (average Pearson correlation: 0.013, $P < 0.01$) (Fig. 5B). This result indicated that the correlation between lncRNAs and their neighboring gene was higher than random coding gene pairs.

Identification of differentially expressed mRNAs, lncRNAs and miRNAs between the high and low fertility groups

From the expression profiles, differentially expressed mRNAs, lncRNAs and miRNAs in the ovaries of Large White pigs were obtained by comparing LH vs. LL and FH vs. FL (Table 2). A total of 956 (345 up-regulated and 611 down-regulated) lncRNA transcripts were differentially expressed in LH vs. LL ($P <$

0.05), while 415 (247 up-regulated and 168 down-regulated) were differentially expressed in FH vs. FL ($P < 0.05$) (Additional file 7: Table S7–1 and 2). We also identified 457 mRNA transcripts that were differentially expressed between the LH and LL groups (Table 2) (Additional file 7: Table S7–3). Among these transcripts, 334 were annotated as known genes. In the FH vs. FL comparison, we found that 475 mRNAs were differentially expressed, while 316 mRNAs were annotated (Additional file 7: Table S7–4). Analyses of the small RNA sequencing data showed that 29 and 11 known miRNAs were differentially expressed when comparing LH vs. LL and FH vs. FL, respectively (Additional file 7: Table S7–5 and 6).

Function enrichment analysis of the lncRNAs

To investigate the function of the differentially expressed lncRNAs in each comparison, the potential targets of lncRNAs were predicted in this study. GO analysis revealed that there were 18 and 15 significant GO terms (corrected $P < 0.05$) in LH vs. LL and FH vs. FL, respectively (Additional file 8: Table S8–1 and 2). We noticed that three significant GO terms were common in all four groups: catalytic activity, single-organism metabolic process and vitamin D metabolic process. The KEGG analysis indicated that a total of 23 and 14 significant pathways were found in LH vs. LL and FH vs. FL, respectively (Additional file 8: Table S8–3 and 4). Importantly, it was observed that “ovarian steroidogenesis” and “lysosome” were the specific enrichment pathways in LH vs. LL, while steroid biosynthesis was the common pathway in the four comparison groups.

Target prediction of miRNAs and construction of miRNA–mRNA networks

To understand the biological functions of differentially expressed miRNAs on fertility, we predicted the potential target genes of these miRNAs in two comparisons. We found that there were 13,458 putative target sites for 122 miRNAs in LH vs. LL and 4,466 target sites for 46 miRNAs in FH vs. FL (Additional file 9: Table S9–1 and 2). Furthermore, GO and pathway enrichment analyses were performed. GO analysis of the target genes revealed that there were 410 and 236 significant GO terms (corrected $P < 0.05$) in LH vs. LL and FH vs. FL comparisons (Additional file 10: Table S10–1 and 2). KEGG pathway analysis revealed that a total of 97 and 31 significant pathways (Hypergeometric Distribution Hypothesis Test, $P < 0.05$) were identified in LH vs. LL and FH vs. FL comparisons, respectively (Additional file 10: Table S10–3 and 4). Among these KEGG pathways, multiple pathways were closely involved in the reproductive process, such as the Insulin signaling pathway, MAPK signaling pathway, Estrogen signaling pathway, GnRH signaling pathway, PI3K-Akt signaling pathway, Ras signaling pathway, Cytokine-cytokine receptor interaction, Jak-STAT signaling pathway and Lysosome pathway in LH vs. LL, and the Notch signaling pathway, TGF-beta signaling pathway and Steroid biosynthesis in FH vs. FL. It is worth noting that the Wnt signaling pathway, Insulin secretion and Adherens junction were common in LH vs. LL and FH vs. FL.

Additionally, we aimed to illustrate negative interactions between differentially expressed miRNAs and mRNAs in the porcine ovary that might lead to differences in fertility; thus, regulatory networks of miRNA–mRNA pairs were constructed (Fig. 6). Of these negative interactions, three miRNAs (ssc-miR-1307, ssc-miR-1343 and ssc-miR-671-5p) targeted multiple mRNAs, but several miRNAs targeted only one mRNA. For example, up-regulated ssc-miR-1307 targets 12 genes, but down-regulated ssc-miR-

361–3p targets only one gene (Fig. 6A). Moreover, down-regulated progestin and adipoQ receptor 7 (*PAQR7*) (FH vs. FL) was regulated by two differentially expressed miRNAs including ssc-miR–885–5p and ssc-miR–671–5p (Fig. 6B).

Construction of lncRNA–miRNA–mRNA networks

To explore the role and relation of lncRNAs and miRNAs mediation in pig fertility, differentially expressed lncRNAs were selected by miRanda analysis. The lncRNA–miRNA negative pairs between differently expressed lncRNAs and miRNAs were selected to construct the co-expression network. In the LH vs. LL comparison, we found that the key miRNAs interacted with 19 lncRNAs (Fig. 7A). In FH vs. FL group, the key miRNAs interacted with 7 lncRNAs (Fig. 7B). A total of 19 and 7 lncRNA–miRNA pairs were identified in LH vs. LL and FH vs. FL, respectively. It is worth noting that most lncRNAs were targeted by the same miRNA. Among these key miRNAs, ssc-miR–1343 and ssc-miR–671–5p had more interactions than others. Ssc-miR–1343 is the key miRNAs targeted with nine key lncRNAs (TCONS_00009287, TCONS_00196796, TCONS_00309415, TCONS_00309419, TCONS_00372560, TCONS_00521720, TCONS_00521721, TCONS_00703255, and TCONS_00814106) through MREs, and ssc-miR–671–5p targeted with six key lncRNAs (TCONS_00019076, TCONS_00229497, TCONS_00429823, TCONS_00651713, TCONS_00702922, and TCONS_00817482), which may be key regulators related to fertility.

Based on the above data, we integrated the lncRNA–miRNA interactions and miRNA–mRNA interactions to establish lncRNA–miRNA–mRNA networks and then visualized using the Cytoscape software (Fig. 8). The network of LH vs. LL was composed of 44 nodes and 40 edges, and the nodes included 4 miRNAs, 14 lncRNAs and 26 mRNAs, which could be the important nodes involved in the ceRNA network during the luteal phase of the estrous cycle (Fig. 8A). In this network, some of them have been reported to be reproduction-associated molecules such as *NUMBL*, *ILF3*, *GRIK4*, *SLC9A1* and *LOXL4*. We noticed that nine lncRNAs were interrelated with ssc-miR–1343 and may act as ceRNA to inhibit target miRNAs and mediated, related hub genes translation such as *NUMBL*, *ILF3*, *TMEM8B*, *PRR14*, *TSHZ2*, and *CAMKV*. In addition, we found that TCONS_00309450 and TCONS_00429684 may serve as ceRNA to mediate *GRIK4* by sponging ssc-miR–1249. In the FH vs. FL group, there were 23 nodes and 22 edges, consisting of 1 miRNA, 6 lncRNAs and 16 mRNAs (Fig. 8B). These six lncRNAs may serve as ceRNA to mediate the corresponding gene transcripts by sponging ssc-miR–671–5p. We also found that several genes, such as *GRIN2D* and *FZD5*, were mainly involved in the “cAMP signaling pathway”, “Calcium signaling pathway”, “Wnt signaling pathway” and “mTOR signaling pathway”, implying that they might be acting as reproduction related genes. Thus, we hypothesize that these lncRNAs, miRNAs and mRNAs play critical roles in fertility regulation.

RT-qPCR Verification

In the lncRNA–miRNA–mRNAs interaction networks, we selected 14 and 5 key nodes to validate expression levels in LH vs. LL and FH vs. FL, respectively, using RT-qPCR (Fig. 9). The expression of each miRNA was significantly higher in the LL groups compared to the LH groups. In contrast, the expression

of each lncRNA or mRNA was significantly lower in the LL groups than in the LH groups (Fig. 9A-D). We also found that the expression of ssc-miR-671-5p was higher in the FL groups compared to the FH groups (Fig. 9E). These results suggested that the post-transcriptional regulatory functions of miRNAs negatively correlated with their targets and that these differentially expressed miRNAs and lncRNAs may contribute to the fertility differences in sows with extreme phenotypes during the follicular and luteal phases of the estrous cycle. In brief, the results demonstrated that the expression patterns of 19 differentially expressed genes were consistent between the RT-qPCR data and the RNA-Seq data, implying that the accuracy of RNA-Seq data was reliable (Fig. 9).

Discussion

Fertility of sows is considered the most important economic trait as it is critical for swine farm profitability. Although a previous report described miRNA expression profiles in pig ovarian tissues correlating with fecundity [25], much less is known about the regulatory molecular mechanisms of fertility in sows. In addition to miRNAs, lncRNAs have been found to play critical roles in transcriptional and post-transcriptional regulation [19]. However, no reports to-date have focused on lncRNA functions in pig fertility. In this study, due to the dynamic nature of the mammalian ovary, we selected ovarian tissues at the follicular and luteal phase to study the differences between the high and low fertility in Large White sows using high throughput sequencing technology. We systematically analyzed the expression of lncRNAs in porcine ovaries, and comprehensively integrated mRNA and miRNA data to identify the lncRNA-miRNA-mRNA interactions mediated in the competing endogenous RNA (ceRNA) network to further elucidate the regulatory mechanisms of lncRNAs in sow fertility.

lncRNAs expression profiles in ovarian tissues at different stages of follicle development in pigs were first investigated using RNA sequencing analysis by Liu et al (2018). In the present study, we used CPC, CNCI, CPAT and Pfam to screen and identify lncRNAs. A total of 24,447 lncRNAs were discovered in the ovarian tissues. We found that the number of lncRNAs detected in this study was much higher than that reported in the study ($n = 2076$) by Liu et al (2018); however, the number was much lower compared to that of human lncRNAs reported in LNCipedia 4.1 [31]. Based on comparative analysis, we observed that the lncRNAs identified in ovarian tissues have fewer exons, lower expression levels, and shorter ORFs than those of the protein-coding genes (Fig. 2B-C and Fig. 3). Our results are consistent with previous studies of thyroid glands and endometriums of pigs [32, 33]. However, our results also showed that the average length of lncRNAs in ovarian tissues were longer than that in the thyroid gland (2,337 bp on average) [32], fetal skeletal muscle (1,043 bp on average) [34] and endometrium of pigs (1,454 bp on average) [33].

As an important post-transcriptional regulatory factor, miRNAs play an essential role in diverse biological processes. In the present study, ssc-miRNA-26a and ssc-miRNA-99a were differentially expressed between the high and low fertility groups in LH vs. LL (Additional file 7: Table S7), which is in accordance with the findings of Huang et al. (2016) [25]. A previous study reported that miR-26a was significantly up-regulated in chicken ovarian follicles and is likely to be associated with the mechanism of recruitment

of dominant follicles [35]. We therefore hypothesize that the two miRNAs may have important roles in reproductive physiology.

Accumulating evidence has demonstrated that miRNAs are important endogenous regulators of gene expression, which have been investigated in various biological mechanisms. However, with the increasing amounts of discovered lncRNAs, the function of very few lncRNAs has been characterized. Recent studies have demonstrated that lncRNAs can act as endogenous miRNA sponges, thereby reducing the negative regulatory effect of miRNAs on mRNAs [36]. Although the ceRNA networks are receiving research attention, most of the relevant studies have focused on their effects related to human diseases.

Apart from miRNAs, lncRNAs in the developing ovary have also been implicated in improving fecundity [27]. However, the potential roles of lncRNAs in regulation of porcine fertility are far from understood. Miao et al. (2016) constructed a miRNA–lncRNA–mRNA interaction network based on the competing endogenous RNA (ceRNA) hypothesis, which provided a new insight into understanding sheep fertility. In the present study, we identified differentially expressed lncRNAs, miRNAs and mRNAs between the high and low fecundity groups in ovarian tissues. Then, we systematically analyzed the complex effects of the interactions between miRNAs and their target genes in LH vs. LL and FH vs. FL groups. Lastly, we constructed new ceRNA networks to comprehensively investigate the potential relationships between lncRNAs and miRNAs in sow fertility.

By constructing lncRNA-miRNA-mRNA regulatory networks using bioinformatics, we identified three miRNAs, ssc-miR-1249, ssc-miR-1307 and ssc-miR-1343, which exhibited significant up-regulation in the LL group compared to the LH group (Fig. 8A). The reliability of their expression patterns was confirmed by RT-qPCR (Fig. 9A, B and D). Among these miRNAs, miR-1249 has been reported to promote the proliferation of glioma cells [37]. Previous work in bull spermatozoa has shown that miR-1249 correlates with fertility rates [38]. The expression of miR-1249 was found to be significantly higher in bulls with moderate fertility compared with the high-fertility group, indicating that miR-1249 negatively regulates the expression of protein-coding genes, which leads to problems during reproduction [38]. Remarkably, miR-1249 was located on *BTA5*, which has been a candidate gene associated with reproduction efficiency in cattle [39]. These results further suggested that miR-1249 might play important roles in fertility regulation. In this network, we determined that the TCONS_00429684/TCONS_00309450–ssc-miR-1249–*GRIK4* interaction axis was involved in the regulatory network. Concerning mRNAs, function enrichment analyses showed that *GRIK4* has been involved in a reproduction-relevant pathway, such as neuroactive ligand-receptor interactions, which play important roles in reproduction processes [40]. In the present study, high levels of *GRIK4* expression was noticed in the LH group compared with the LL group. Meanwhile, the RT-qPCR results also revealed that the expression pattern of *GRIK4* was consistent with TCONS_0042968. However, the expression of ssc-miR-1249 was significantly increased in the LL group, which means that it might inhibit the transcription of *GRIK4* and exert a negative impact on the fertility of pigs. Thus, we speculate that the high expression of lncRNAs (TCONS_00429684 and TCONS_00309450) in the LH group may be through the absorption

of ssc-miR-1249 to promote *GR/K4* transcription. Despite our observations, the underlying mechanisms need further investigation.

We also found that ssc-miR-1343 and ssc-miR-1307 played central roles in the regulation network (Fig. 6A). No previous study has reported the expression of ssc-miR-1307 and ssc-miR-1343 in ovarian tissue. According to our results, ssc-miR-1307 and ssc-miR-1343 showed significant up-regulation in the LL group. The RT-qPCR results revealed that the expression patterns of Interleukin Enhancer Binding Factor 3 (*ILF3*) and Numblike (*NUMBL*) were consistent with several lncRNAs (Fig. 8A). Some studies showed that *ILF3* is strongly expressed in the mouse ovary and that the *ILF3* protein predominantly functions in germ cells [41]. The *ILF3* protein was frequently detected in adult zebra fish gonads by global proteomics [42], and may be involved in gonad differentiation [43]. In addition, the Notch signaling pathway could be involved in the development of organs and tissues by regulating cellular developmental processes, such as cell proliferation, differentiation and apoptosis [44]. A recent publication by Jing et al. (2017) reported that the Notch signaling pathway could promote ovarian follicular development by regulating the growth and estradiol production of granulosa cells [45]. *NUMBL*, a known antagonist of Notch signaling, has been implicated in gonadal development. Research has confirmed that deletion of *NUMBL* disrupted coelomic epithelium cell polarity in both XX and XY gonads, and germ cell numbers were also reduced at early stages of gonadogenesis, suggesting a major role in gonad development [46]. In this study, ssc-miR-1343 had the most interactions in the network, which is a bridge of *ILF3*, *NUMBL* and several lncRNAs. Based on the combined detection of their expression, we speculate that these lncRNAs might be associated with reproductive efficiency in sows.

In addition to FH vs. FL, we analyzed the relationship among lncRNAs, miRNAs, and mRNAs in ovarian tissues, as shown in Fig. 6B. We found that miR-671-5p had the most interactions, indicating that it is the hub gene in the regulation network. We further observed that miR-671-5p potential target gene *FZD5* was largely involved in the Wnt and mTOR signaling pathways, which plays a critical role during the estrous cycle [47, 48]. Specifically, the TCONS_00019076-miR-671-5p-FZD5 interaction is involved in the regulatory network. The RT-qPCR results revealed that the expression of *FZD5* was significantly up-regulated in the FH groups, which was consistent with the results from the RNA-seq data. Furthermore, we showed that the level of TCONS_00019076 was up-regulated in the LH groups, which was consistent with the expression pattern of *FZD5*. Given the potential binding sites between TCONS_00019076- miR-671-5p and miR-671-5p-FZD5, we propose that TCONS_00019076 may promote the expression of *FZD5* through the absorption of miR-671-5p. In addition, two of the 16 mRNAs, *PAQR7* and *IGF2BP2*, have been reported to be related to oocyte maturation and cell proliferation [49, 50]. Thus, we suggest that these key lncRNAs may play an important role in the regulation of pig fertility. In future research, we plan to explore the function of these lncRNAs using overexpression and knockdown experiments.

Conclusions

In this study, ovarian lncRNAs and miRNAs associated with prolificacy of Large White sows were identified during the follicular and luteal phases of the estrous cycle, and their potential biological

functions were predicted through bioinformatics. In addition, we constructed interaction networks among a series of differentially expressed lncRNAs, miRNAs, and mRNAs in ovarian tissues using an integrative biology approach. Our data will be helpful for identifying a novel regulatory mechanism for investigating prolificacy in pigs in future studies.

Methods

Swine population pool, experimental design and tissue collection

Detailed documents of 590 multiparous Canadian Large White cyclic sows were obtained from the Hebei Shunde-Tianzhao Livestock Technology Co., Ltd, Wanquan, Hebei, China. For this study, total number of piglets born (TNB) was regarded as an important parameter to evaluate the fertility of the animals. TNB was calculated using the SPSS19.0 software package (IBM Corp, Armonk, NY, USA). The average TNB was 13.42 piglets, the 10% lower tail probability was 11.11 piglets and the 10% upper tail probability was 15.73 piglets per litter. Based on the criteria stated above, sows were divided into two groups: high (H; TNB > 15.73) and low (L; TNB < 11.11) fertility. Then, eight sows with similarly high or low parity from each group were chosen for the study ($n = 8$ for the H group and $n = 8$ for the L group). All phenotypic records are listed in Table 1. Given the importance of ovarian activities, ovaries in luteal (L) or follicular (F) phases of the estrous cycle [51] were analyzed for the differences between H and L fertility sows. Sows with H and L fertility were sacrificed at each of the two stages: on day 14 (day 1 = first day of estrus) after estrus in the L phase ($n = 4$ for H fertility sows during the L phase [LH] and $n = 4$ for L fertility sows during the L phase [LL]) and on day 20 of the estrous cycle in the follicular phase ($n = 4$ for H fertility sows during the F phase [FH] and $n = 4$ for L fertility sows during the F phase [FL]). At the above time points, animals were humanely slaughtered by electronic stunning followed by exsanguinations, and the ovarian tissues were rapidly removed and snap-frozen in liquid nitrogen until subsequent processing. All animal experiments were performed in accordance with the Institutional Animal Care and Use Committee at the Hebei Agricultural University (Baoding, People's Republic of China). All experiments were conducted in accordance with the regulations and guidelines established by that committee.

RNA extraction and qualification

Total RNA was extracted from each ovarian sample using TRIzol Reagent (Invitrogen, Carlsbad, CA, USA), purified with RNeasy Mini Kit (Qiagen, Valencia, CA, USA). Total RNA from each sample was then quantified and qualified by an Agilent 2100 Bio-analyzer (Agilent Technologies, Palo Alto, CA, USA), NanoDrop (Thermo Fisher Scientific Inc, Waltham, MA, USA) and 1% agarose gel. Samples with an RNA Integrity Number (RIN) value > 7.5 were used for library preparation. The same sample was used for both sequencing and RT-qPCR analysis.

Library preparation and solexa sequencing

Approximately 3 μ g of RNA of each RNA sample was used for library preparations. To remove ribosomal RNA (rRNA), the Epicentre Ribo-ZeroTM rRNA removal Kit (Epicentre, Madison, WI, USA) was used. Then, the

rRNA-depleted RNA was used to generate cDNA libraries using the NEBNext® Ultra™ The Directional RNA Library Prep Kit for Illumina® (New England Biolabs;NEB, Ipswich, MA, USA) according to the manufacturer's protocol. The first cDNA strand was synthesized using ProtoScript II Reverse Transcriptase (NEB). Next, the second-strand DNA strand was synthesized using a Second Strand Synthesis Enzyme Mix (including dACG-TP/dUTP) (NEB). Subsequently, the purified double-stranded DNA was ligated to adaptors, after being end-repaired and A-tailed. Approximately 300 bp cDNA fragments were isolated. The dUTP-marked second strand was digested with an Uracil-Specific Excision Reagent (USER) enzyme (NEB). Finally, each sample was amplified by PCR to enrich cDNA libraries. Sequencing was carried out using a 2×150 paired-end (PE) configuration on Illumina HiSeq X10 (Illumina, San Diego, CA, USA) by GENEWIZ (Suzhou, China).

For small RNA sequencing, the same samples were used to construct Illumina small RNA-Seq (RNA sequencing) libraries using the NEBNext® Multiplex Small RNA library Prep Set for Illumina® (NEB) following the manufacturer's recommendations. In brief, 3' SR Adaptor for Illumina was ligated to the small RNA using 3' Ligation Enzyme. The 5' SR Adaptor for Illumina was ligated to the small RNA using 5' Ligation Enzyme and first strand cDNA was synthesized using ProtoScript II Reverse Transcriptase (NEB). Each sample was then amplified by PCR for 12 cycles using P5 and P7 primers, with both primers carrying sequences which can anneal with flow cell to perform bridge PCR and P7 primers carrying a six-base index, thus allowing multiplexing. The PCR products of ~140 bp were recovered and cleaned up using PAGE. Purified small RNA sequencing libraries were validated using an Agilent 2100 Bioanalyzer (Agilent Technologies, Palo Alto, CA, USA), and quantified by a Qubit 2.0 Fluorometer (Invitrogen). Finally, the 16 small RNA libraries were sequenced using a 1×50 single-end (SE) sequencing strategy by Illumina HiSeq X10 (Illumina).

Analysis of RNA-Seq data

Raw RNA-seq reads from each sample were first processed by removing adapters and low-quality reads. Clean data from each library were obtained and then mapped to the reference genome (Sscrofa10.2) that was downloaded from the Ensembl Genomes (<http://www.ensemblgenomes.org>) using Hisat2 (v2.0.1). The mapped reads were assembled using StringTie V1.0.4 [52]. Additionally, the assembled transcripts from each individual animal were merged with Cuffmerge to generate a single transcriptome annotation from Ensembl. Rsem (V1.2.6) [53] was used to calculate gene expression levels using the FPKM (Fragments per Kilo bases per Million reads) method for both the lncRNAs and coding genes in each sample. Differential expression analysis was performed using the DESeq2 package (v1.6.3) (2013, Anders and Huber, European Molecular Biology Laboratory [EMBL], Heidelberg, Germany); a model based on the negative binomial distribution. Following adjustment by Benjamini and Hochberg's approach [54, 55] for controlling false discovery rate, transcripts of genes showing *P* values < 0.05 and with a $|log_2(\text{fold change})| \geq 1$ were treated as differentially expressed. The sequencing data obtained from RNA-seq were released to the National Center for Biotechnology Information (NCBI) Gene Expression Omnibus (GEO) database under the accession number GSE134001.

Analysis of microRNA-Seq data (miRNA)

Raw reads from the 16 small RNA libraries were generated. Clean reads were obtained by masking adapters, poly-A tails and low-quality reads from the raw data with Trimmomatic10 (v0.30) [56]. The clean reads were subsequently mapped to the reference sequence by Bowtie [52]. They were then aligned to the porcine genome sequence (Sscrofa10.2) by Bowtie2 (v2.1.0). Subsequently, unmapped reads were used to predict the novel miRNAs with miRDeep (v2.0.0.7) [57]. Differential expression analysis used the DEseq2 package, a model based on the negative binomial distribution. Following adjustment by Benjamini and Hochberg's approach for controlling the false discovery rate, *P* values of miRNAs were settled at < 0.05 and $|\log_2(\text{fold change})| \geq 1$ were described to detect differentially expressed miRNAs. The sequencing data obtained from RNA-seq were released to the National Center for Biotechnology Information (NCBI) Gene Expression Omnibus (GEO) database under the accession number GSE132307.

Target prediction of miRNAs and construction of miRNA–mRNA networks

To explore the function of the miRNA, potential target genes of miRNAs with differential abundances were predicted by miRanda [58]. Subsequently we utilized GO-TermFinder (v0.86) (<https://metacpan.org/release/GO-TermFinder>) to identify Gene Ontology (GO) terms that annotated a list of enriched genes with a significant *P* value less than 0.05. The enrichment of KEGG pathways was tested using in-house scripts. In order to explore the potential interactions of miRNA and mRNA, miRNA–mRNA negative interactions were predicted, and Cytoscape_v3.5.1 [59] was used to construct the important networks of differentially expressed mRNAs and miRNAs.

lncRNAs identification

According to the characteristics of the lncRNA, all the assembled transcripts were merged and then filtered by known non-lincRNA annotation, non-lincRNA characters, open reading frames (ORFs) and protein-coding potential methods. Known non-lincRNA include known protein-coding RNA, miRNA, tRNA, snoRNA, rRNA and pseudogenes. The characters of non-lincRNA include transcripts with more than one exon and with a length > 200 bp. For protein-coding potential prediction, we used CPC (Coding Potential Calculator) [60], CNCI (coding-noncoding-index) [61], CPAT (coding potential assessment tool) [62] and Pfam-scan [63] to distinguish mRNAs from lncRNAs. To understand the differences between lncRNAs and mRNAs, the genomic features of the predicted lncRNAs were analyzed [64].

LncRNAs target gene prediction and GO and KEGG enrichment analyses

Transcriptional regulation by lncRNAs can work either in cis or in trans and may negatively or positively control gene expression [65]. As a result, the prediction of lncRNA target genes in cis and trans forms were performed. We searched coding genes 10k upstream and downstream regions of lncRNAs as the cis target gene using Bedtools (v2.17.0). Regulation in trans was analyzed by expression levels, according to Pearson's correlation coefficient ($|r| > 0.95$).

To investigate the function of differentially expressed lncRNAs, GO enrichment analysis was performed using GO-TermFinder (v0.86) (<https://metacpan.org/release/GO-TermFinder>), and corrected *P* values < 0.05 were treated as significantly enriched. KEGG pathway analysis was implemented using in-house scripts.

Construction of lncRNA–miRNA–mRNA networks

To infer the function of lncRNAs, differently expressed lncRNAs were selected, and then lncRNA–miRNA negative interactions were predicted using miRanda [66]. Subsequently, based on complementary pairs between miRNA and mRNAs and between miRNAs and lncRNAs, the lncRNA–miRNA–mRNA interaction networks were constructed and visualized by Cytoscape_v3.5.1 [59].

Reverse transcription real-time quantitative PCR (RT-qPCR)

To validate sequencing data accuracy, RT-qPCR was conducted based on the lncRNA–miRNA–mRNA correlation networks. Specifically, several interaction nodes were validated by RT-qPCR. For mRNA and lncRNA, reverse transcription of total RNA was performed using a Thermo First Strand cDNA Synthesis Kit (Sinogene, Beijing, China) with random primers included in the kit. Quantitative PCR was carried out with SYBR Green qPCR Mix (Sinogene, Beijing, China) on StepOne real-time PCR systems (Applied Biosystems, Carlsbad, CA, USA). All amplifications were followed by dissociation curve analysis of the amplified products. For miRNA, reverse transcription of total RNA was performed using a One-Step miRNA RT Kit (Sinogene). The reactions were performed on StepOne real-time PCR systems (Applied Biosystems) using SYBR Green qPCR Mix (Sinogene). All primer sequences, including selected genes, miRNAs and internal control genes (ACTB and U6 snRNA), are displayed in Additional file 1: Table S1. Relative expression levels of genes and miRNAs were calculated by the $2^{-\Delta\Delta Ct}$ method [67].

Statistical analysis

Statistical analyses were performed using SPSS 19.0 statistical software (IBM Corp). The data are expressed as the mean \pm standard deviation (SD) of three independent experiments. When comparisons were made, Student's *t*-tests were performed, and *P* < 0.05 was considered as statistically significant.

Abbreviations

lncRNAs: long noncoding RNAs; miRNAs: micro RNAs; RNA-seq: RNA sequencing; MREs: miRNA response elements; RT-qRCR: Reverse Transcription Real-time Quantitative PCR; ceRNAs: competing endogenous RNAs; TNB: total number of piglets born; RIN: RNA Integrity Number; FPKM: Fragments per Kilo bases per Million reads; PAQR7: progestin and adiponectin receptor 7; GRIK4: glutamate receptor, ionotropic, kainate 4; ILF3: Interleukin Enhancer Binding Factor 3.

Declarations

Ethics approval and consent to participate

All animal experiments were performed in accordance with the Institutional Animal Care and Use Committee at the Hebei Agricultural University (Baoding, People's Republic of China). All experiments were conducted in accordance with the regulations and guidelines established by that committee.

Consent for publication

Not applicable.

Availability of data and materials

The datasets generated for this study can be found in the National Center for Biotechnology Information (NCBI) Gene Expression Omnibus (GEO) database, Accession numbers GSE134001 and GSE132307.

Competing interests

The authors declare that they have no competing interests.

Funding

This work was supported by a grant from the Modern Agriculture Industry Technology System Foundation of Hebei Province (grant # HBCT2018110201). The funding body didn't participate in the design of the study, collection, analysis and interpretation of data or in writing the manuscript.

Author Contributions

HYH performed the research, analyzed the data, and wrote the manuscript; QJ conceived the study and was involved in its design and coordination; JZX and BZ were involved in the design of the study. ZQL performed the statistical analysis; QJ reviewed the manuscript. All authors edited and approved the final manuscript.

Acknowledgments

We thank LetPub (www letpub com) for its linguistic assistance during the preparation of this manuscript.

Author details

¹Department of Animal Genetics, Breeding and Reproduction, College of Animal Science and Technology, Hebei Agricultural University, Baoding 071000, Hebei, China. ²Engineering Research Center for Agriculture in Hebei Mountainous Areas, Baoding 071000, Hebei, China

References

1. Cassady JP, Johnson RK, Pomp D, Rohrer GA, Van Vleck LD, Spiegel EK, et al. Identification of quantitative trait loci affecting reproduction in pigs. *J Anim Sci.* 2001; 79(3):623–633.
2. Li K, Ren J, Xing Y, Zhang Z, Ma J, Guo Y, et al. Quantitative trait loci for litter size and prenatal loss in a White Duroc x Chinese Erhualian resource population. *Anim Genet.* 2009; 40(6): 963–966.
3. Bergfelder-Drüing S, Grosse-Brinkhaus C, Lind B, Erbe M, Schellander K, Simianer H, et al. A genome-wide association study in large white and landrace pig populations for number piglets born alive. *PLoS One.* 2015; 10(3): e0117468.
4. Wang Y, Ding X, Tan Z, Xing K, Yang T, Wang Y, et al. (2018). Genome-wide association study for reproductive traits in a Large White pig population. *Anim Genet.* 2018; 49(3):127–131.
5. Uzzaman MR, Park JE, Lee KT, Cho ES, Choi BH, Kim TH. A genome-wide association study of reproductive traits in a Yorkshire pig population. *Livest Sci.* 2018; 209:67–72.
6. Metodiev S, Thekkoot DM, Young JM, Onteru S, Rothschild MF, Dekkers JCM. et al. A whole-genome association study for litter size and litter weight traits in pigs. *Livest Sci.* 2018; 211: 87–97.
7. Hu ZL, Park CA, Reecy JM. Developmental progress and current status of the animal QTLdb. *Nucleic Acids Res.* 2016; 44(D1):D827–D833.
8. Carninci P, Kasukawa T, Katayama S, Gough J, Frith MC. The transcriptional landscape of the mammalian genome. *Science.* 2005; 309(5740):1559–1563.
9. Salhi A, Essack M, Alam T, Bajic VP, Ma L, Radovanovic A, et al. DES-ncRNA: A knowledgebase for exploring information about human micro and long noncodingRNAs based on literature-mining. *RNA Biol.* 2017; 14(7): 963–971.
10. Ponting CP, Oliver PL, Reik W. Evolution and functions of long noncoding RNAs. *Cell.* 2009; 136(4): 629–641.
11. Mas-Ponte D, Carlevaro-Fita J, Palumbo E, Pulido TH, Guigo R, Johnson R. LncATLAS database for subcellular localization of long noncoding RNAs. *RNA.* 2017; 23(7):1080–1087.
12. Hu G, Niu F, Humburg BA, Liao K, Bendi VS, Callen S, et al. Molecular mechanisms of long noncoding RNAs and their role in disease pathogenesis. *Oncotarget.* 2018; 9(26):18648–18663.
13. Gong QY, Su GF. Roles of miRNAs and long noncoding RNAs in the progression of diabetic retinopathy. *Biosci Rep.* 2017; 37(6): BSR20171157.
14. Van Roosbroeck K, Pollet J, Calin GA. miRNAs and long noncoding RNAs as biomarkers in human diseases. *Expert Rev Mol Diagn.* 2013; 13(2):183–204.

15. Pradeepa MM, McKenna F, Taylor GC, Bengani H, Grimes GR, Wood AJ, et al. Psip1/p52 regulates posterior Hoxa genes through activation of lncRNA Hottip. *PLoS Genet.* 2017; 13(4):e1006677.
16. Yan ZQ, Huang XY, Sun WY, Yang QL, Shi HR, Jiang TT, et al. Analyses of long non-coding RNA and mRNA profiling in the spleen of diarrheic piglets caused by Clostridium perfringens type C. *Peer J.* 2018; 6: e5997.
17. Salmena L, Poliseno L, Tay Y, Kats L, Pandolfi PP. A ceRNA hypothesis: the Rosetta Stone of a hidden RNA language?. *Cell.* 2011; 146(3):353–358.
18. Tao H, Zhang JG, Qin RH, Dai C, Shi P, Yang JJ, et al. LncRNA GAS5 controls cardiac fibroblast activation and fibrosis by targeting miR-21 via PTEN/MMP-2 signaling pathway. *Toxicology.* 2017; 386:11–18.
19. Li Y, Chen X, Sun H, Wang H. Long non-coding RNAs in the regulation of skeletal myogenesis and muscle diseases. *Cancer Lett.* 2018; 417:58–64.
20. Song YX, Sun JX, Zhao JH, Yang YC, Shi JX, Wu ZH, et al. Non-coding RNAs participate in the regulatory network of CLDN4 via ceRNA mediated miRNA evasion. *Nat Commun.* 2017; 8(1):289.
21. Liang H, Yu T, Han Y, Jiang H, Wang C, You T, et al. LncRNA PTAR promotes EMT and invasion-metastasis in serous ovarian cancer by competitively binding miR-101-3p to regulate ZEB1 expression. *Mol Cancer.* 2018; 17(1):119.
22. Donadeu FX, Schauer SN, Sontakke SD. Involvement of miRNAs in ovarian follicular and luteal development. *J Endocrinol.* 2012; 215(3):323–334.
23. Hsueh AJ, Kawamura K, Cheng Y, Fauser BC. Intraovarian Control of Early Folliculogenesis. *Endocr Rev.* 2015; 36(1):1–24.
24. Li MZ, Liu YK, Wang T, Guan JQ, Luo ZG, Chen HS, et al. Repertoire of porcine microRNAs in adult ovary and testis by deep sequencing. *Int J Biol Sci.* 2011; 7(7):1045–1055.
25. Huang L, Yin ZJ, Feng Y, Zhang XD, Wu T, Ding YY, et al. Identification and differential expression of microRNAs in the ovaries of pigs (*Sus scrofa*) with high and low litter sizes. *Anim Genet.* 2016; 47(5):543–551.
26. Miao XY, Luo QM, Zhao HJ, Qin XY. Genome-wide analysis of miRNAs in the ovaries of Jining Grey and Laiwu Black goats to explore the regulation of fecundity. *Sci Rep.* 2016; 6:37983.
27. Miao XY, Luo QM, Zhao HJ, Qin XY. Ovarian transcriptomic study reveals the differential regulation of miRNAs and lncRNAs related to fecundity in different sheep. *Sci Rep.* 2016; 6:35299.
28. Tang Z, Wu Y, Yang Y, Yang YT, Wang Z, Yuan J, et al. Comprehensive analysis of long non-coding RNAs highlights their spatio-temporal expression patterns and evolutionary conservation in *Sus scrofa*. *Sci Rep.* 2017; 7:43166.
29. Liu Y, Li M, Bo X, Li T, Ma L, Zhai T, et al. Systematic Analysis of Long Non-Coding RNAs and mRNAs in the Ovaries of Duroc Pigs During Different Follicular Stages Using RNA Sequencing. *Int J Mol Sci.* 2018; 19(6):E1722.

30. Guttman M, Garber M, Levin JZ, Donaghey J, Robinson J, Adiconis X, et al. Ab initio reconstruction of cell type-specific transcriptomes in mouse reveals the conserved multi-exonic structure of lincRNAs. *Nat Biotechnol.* 2010; 28(5):503–510.
31. Volders PJ, Verheggen K, Menschaert G, Vandepoele K, Martens L, Vandesompele J, et al. An update on LNCipedia: a database for annotated human lncRNA sequences. *Nucleic Acids Res.* 2015; 43(D1):D174-D180.
32. Shen Y, Mao H, Huang M, Chen L, Chen J, Cai Z, et al. Long Noncoding RNA and mRNA Expression Profiles in the Thyroid Gland of Two Phenotypically Extreme Pig Breeds Using Ribo-Zero RNA Sequencing. *Genes.* 2016; 7(7):34.
33. Wang Y, Xue S, Liu X, Liu H, Hu T, Qiu X, et al. Analyses of Long Non-Coding RNA and mRNA profiling using RNA sequencing during the pre-implantation phases in pig endometrium. *Sci Rep.* 2016; 6:20238.
34. Zhao W, Mu Y, Ma L, Wang C, Tang Z, Yang S, et al. Systematic identification and characterization of long intergenic non-coding RNAs in fetal porcine skeletal muscle development. *Sci Rep.* 2015; 5:8957.
35. Kang L, Cui X, Zhang Y, Yang C, Jiang Y. Identification of miRNAs associated with sexual maturity in chicken ovary by Illumina small RNA deep sequencing. *BMC Genomics.* 2013; 14:352.
36. Tay Y, Rinn J, Pandolfi PP. The multilayered complexity of ceRNA crosstalk and competition. *Nature.* 2014; 505(7483):344–352.
37. Fang B, Li G, Xu C, Hui Y, Li G. MicroRNA miR-1249 downregulates adenomatous polyposis coli 2 expression and promotes glioma cells proliferation. *Am J Transl Res.* 2018; 10(5):1324–1336.
38. Fagerlind M, Stalhammar H, Olsson B, Klinga-Levan K. Expression of miRNAs in Bull Spermatozoa Correlates with Fertility Rates. *Reprod Domest Anim.* 2015; 50(4):587–594.
39. McDaneld TG, Kuehn LA, Thomas MG, Snelling WM, Smith E TP, Pollak EJ, et al. Genome wide association study of reproductive efficiency in female cattle. *J Anim Sci.* 2014; 92(5):1945–1957.
40. Sahu DK, Panda SP, Meher PK, Das P, Routray P, Sundaray JK, et al. Construction, De-Novo Assembly and Analysis of Transcriptome for Identification of Reproduction-Related Genes and Pathways from Rohu, Labeo rohita (Hamilton). *PLoS One.* 2015; 10(7): e0132450.
41. Buaas FW, Lee K, Edelhoff S, Disteche C, Braun RE. Cloning and characterization of the mouse interleukin enhancer binding factor 3 (Ilf3) homolog in a screen for RNA binding proteins. *Mamm Genome.* 1999; 10(5):451–456.
42. Groh KJ, Nesatyy VJ, Segner H, Eggen RI, Suter MJ. Global proteomics analysis of testis and ovary in adult zebrafish (*danio rerio*). *Fish Physiol Biochem.* 2011; 37(3):619–647.
43. Groh KJ, Schönenberger R, Eggen RI, Segner H, Suter MJ. Analysis of protein expression in zebrafish during gonad differentiation by targeted proteomics. *Gen Comp Endocrinol.* 2013; 193, 210–220.
44. Li HS, Wang D, Shen Q, Schonemann MD, Gorski JA, Jones KR, et al. Inactivation of numb and numblike in embryonic dorsal forebrain impairs neurogenesis and disrupts cortical morphogenesis. *Neuron.* 2003; 40(6):1105–1118.

45. Jing J, Jiang X, Chen J, Yao X, Zhao M, Li P, et al. Notch signaling pathway promotes the development of ovine ovarian follicular granulosa cells. *Anim Reprod Sci.* 2017; 181:69–78.
46. Lin YT., Barske L, DeFalco T, Capel B. Numb regulates somatic cell lineage commitment during early gonadogenesis in mice. *Development.* 2017; 144(9):1607–1618.
47. Atli MO, Guzeloglu A, Dinc DA. Expression of wingless type (WNT) genes and their antagonists at mRNA levels in equine endometrium during the estrous cycle and early pregnancy. *Anim Reprod Sci.* 2011; 125(1–4):94–102.
48. Zavareh S, Gholizadeh Z, Lashkarbolouki T. Evaluation of changes in the expression of Wnt/β-catenin target genes in mouse reproductive tissues during estrous cycle: An experimental study. *Int J Reprod Biomed (Yazd).* 2018; 16(2):69–76.
49. Shi B, Liu X, Thomas P, Pang Y, Xu Y, Li X, et al. Identification and characterization of a progestin and adipoQ receptor (PAQR) structurally related to Paqr7 in the ovary of *Cynoglossus semilaevis* and its potential role in regulating oocyte maturation. *Gen Comp Endocrinol.* 2016; 237:109–120.
50. Haouzi D, Assou S, Monzo C, Vincens C, Dechaud H, Hamamah S. Altered gene expression profile in cumulus cells of mature MII oocytes from patients with polycystic ovary syndrome. *Hum Reprod.* 2012; 27(12):3523–3530.
51. Soede NM, Langendijk P, Kemp B. Reproductive cycles in pigs. *Anim Reprod Sci.* 2011; 124(3–4):251–258.
52. Langmead B, Trapnell C, Pop M, Salzberg SL. Ultrafast and memory-efficient alignment of short DNA sequences to the human genome. *Genome Biol.* 2009; 10(3):R25.
53. Mortazavi A, Williams BA, McCue K, Schaeffer L, Wold B. Mapping and quantifying mammalian transcriptomes by RNA-Seq. *Nat Methods.* 2008; 5(7):621–628.
54. Audic S, Claverie JM. The significance of digital gene expression profiles. *Genome Res.* 1997; 7(10):986–995.
55. Benjamini Y, Yekutieli D. The control of the false discovery rate in multiple testing under dependency. *Ann. Stat.* 2001; 29(4):1165–1188.
56. Bolger AM, Lohse M, Usadel B. Trimmomatic: a flexible trimmer for Illumina sequence data. *Bioinformatics.* 2014; 30(15):2114–2120.
57. Friedländer MR, Chen W, Adamidi C, Maaskola J, Einspanier R, Knespel S, et al. Discovering microRNAs from deep sequencing data using miRDeep. *Nat Biotechnol.* 2008; 26(4):407–415.
58. Rajewsky N. microRNA target predictions in animals. *Nat Genetics.* 2006; 38:S8–13.
59. Shannon P, Markiel A, Ozier O, Baliga NS, Wang JT, Ramage D, et al. Cytoscape: a software environment for integrated models of biomolecular interaction networks. *Genome Res.* 2003; 13(11):2498–2504.
60. Kong L, Zhang Y, Ye ZQ, Liu XQ, Zhao SQ, Wei L, et al. CPC: assess the protein-coding potential of transcripts using sequence features and support vector machine. *Nucleic Acids Res.* 2007; 35:W345–349.

61. Sun L, Luo H, Bu D, Zhao G, Yu K, Zhang C, et al. Utilizing sequenceintrinsic composition to classify protein-coding and long non-coding transcripts. *Nucleic Acids Res.* 2013; 41(17):e166.
62. Wang L, Park HJ, Dasari S, Wang S, Kocher JP, Li W. CPAT: Coding-Potential Assessment Tool using an alignment-free logistic regression model. *Nucleic Acids Res.* 2013; 41(6):e74.
63. Bateman A, Birney E, Cerruti L, Durbin R, Etwiller L, Eddy SR, et al. The Pfam protein families database. *Nucleic Acids Res.* 2002; 30:276–280.
64. Siepel A, Bejerano G, Pedersen JS, Hinrichs AS, Hou M, Rosenbloom K, et al. Evolutionarily conserved elements in vertebrate, insect, worm, and yeast genomes. *Genome Res.* 2005; 15(8):1034–1050.
65. Carmona S, Lin B, Chou T, Arroyo K, Sun S. LncRNA Jpx induces Xist expression in mice using both trans and cis mechanisms. *PLoS Genet.* 2018; 14(5):e1007378.
66. Betel D, Koppal A, Agius P, Sander C, Leslie C. Comprehensive modeling of microRNA targets predicts functional non-conserved and non-canonical sites. *Genome Biol.* 2010; 11(8):R90.
67. Livak KJ, Schmittgen TD. Analysis of relative gene expression data using real-time quantitative PCR and the 2-Delta Delta C (T) Method. *Methods.* 2001; 25(4):402–408.

Tables

Table 1. Phenotypic records of Danish LargeWhite sows used in this study

Group	Sample ID	Parities	TNB ^c	NBA ^d	Estrous cycle
LH ^a	LH1	6	17.00±1.45	15.85±0.92	Luteal phase
	LH2	6	16.00±1.51	14.71±1.20	
	LH3	5	15.50±1.85	14.90±0.82	
	LH4	5	16.20±2.01	14.56±1.02	
LL ^a	LL1	4	9.50±1.84	8.70±0.70	
	LL2	4	7.33±1.64	7.0±0.34	
	LL3	3	9.33±1.92	8.92±0.43	
	LL4	3	9.67±2.10	8.74±1.05	
FH ^b	FH1	4	12.33±2.12	11.2±0.72	Follicular phase
	FH2	7	16.71±1.39	15.83±1.38	
	FH3	7	16.57±1.39	14.67±1.05	
	FH4	4	17.00±1.84	15.94±0.86	
FL ^b	FL1	4	6.00±1.84	5.20±0.51	
	FL2	3	8.33±2.12	7.92±0.40	
	FL3	3	4.67±2.60	4.67±2.60	
	FL4	3	8.33±2.12	7.30±0.72	

^aLH and LL represent Large White sows with high and low litter sizes, respectively, during the luteal phase of the estrous cycle; ^bFH and FL represent pigs with high and low litter sizes, respectively, during the follicular phase. ^cTNB: Total number of piglets born. ^dNBA: Numberborn alive. Values are the mean ± SD.

Table 2. Number of differentially expressed genes in LH vs. LL and FH vs. FL

Genes	LH vs. LL		Total	FH vs. FL		Total
	Up-regulated	Down-regulated		Up-regulated	Down-regulated	
mRNAs	161	296	457	253	222	475
lncRNAs	345	611	956	247	168	415
miRNAs	68	54	122	32	14	46

Figures

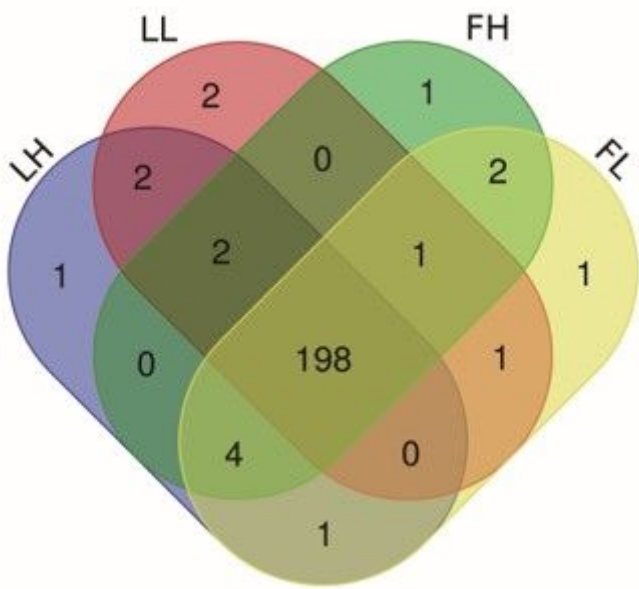


Figure 1

Venn diagrams of miRNAs. A total of 198 known miRNAs were shared in four groups (LH, LL, FH and FL).

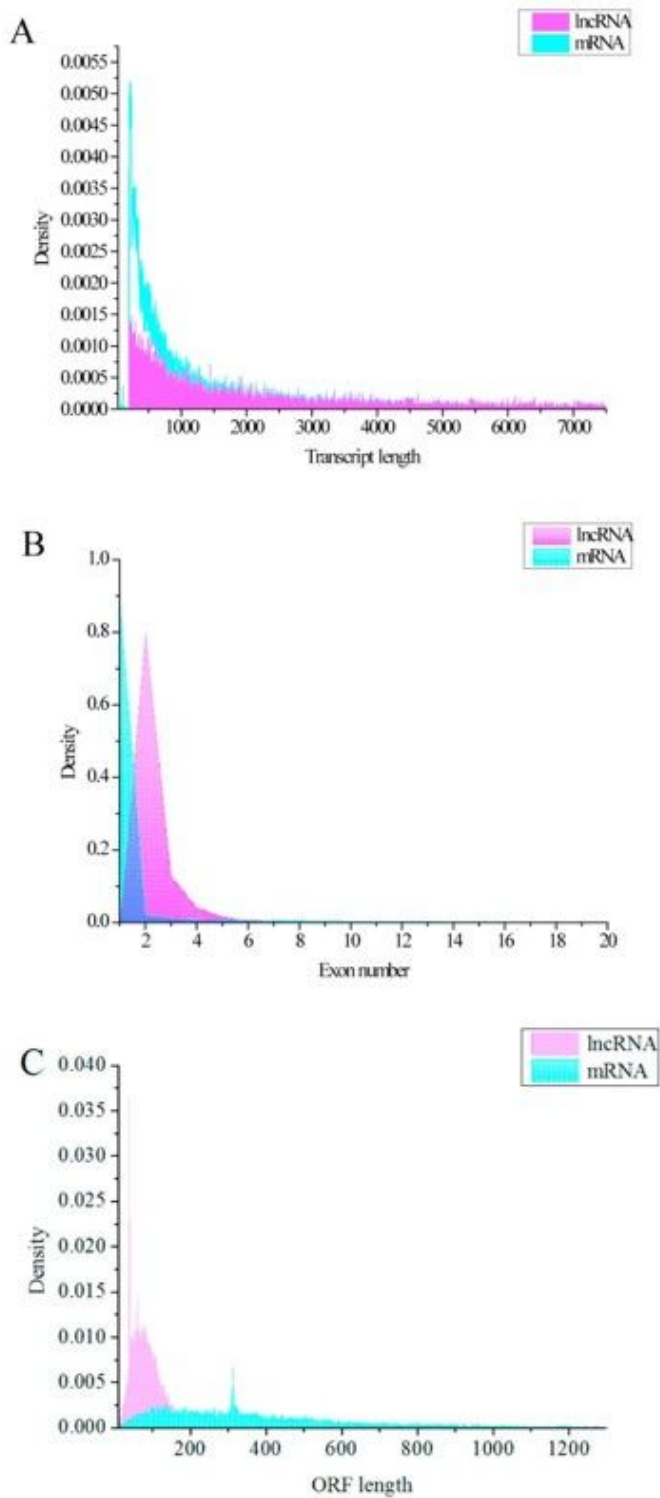


Figure 2

Genomic features of lncRNAs. (A) Length distribution of 27,370 mRNAs (pink) and 24,447 lncRNAs (blue). (B) Exon number distribution of mRNAs and lncRNAs. (C) ORF length distribution of mRNAs and lncRNAs.

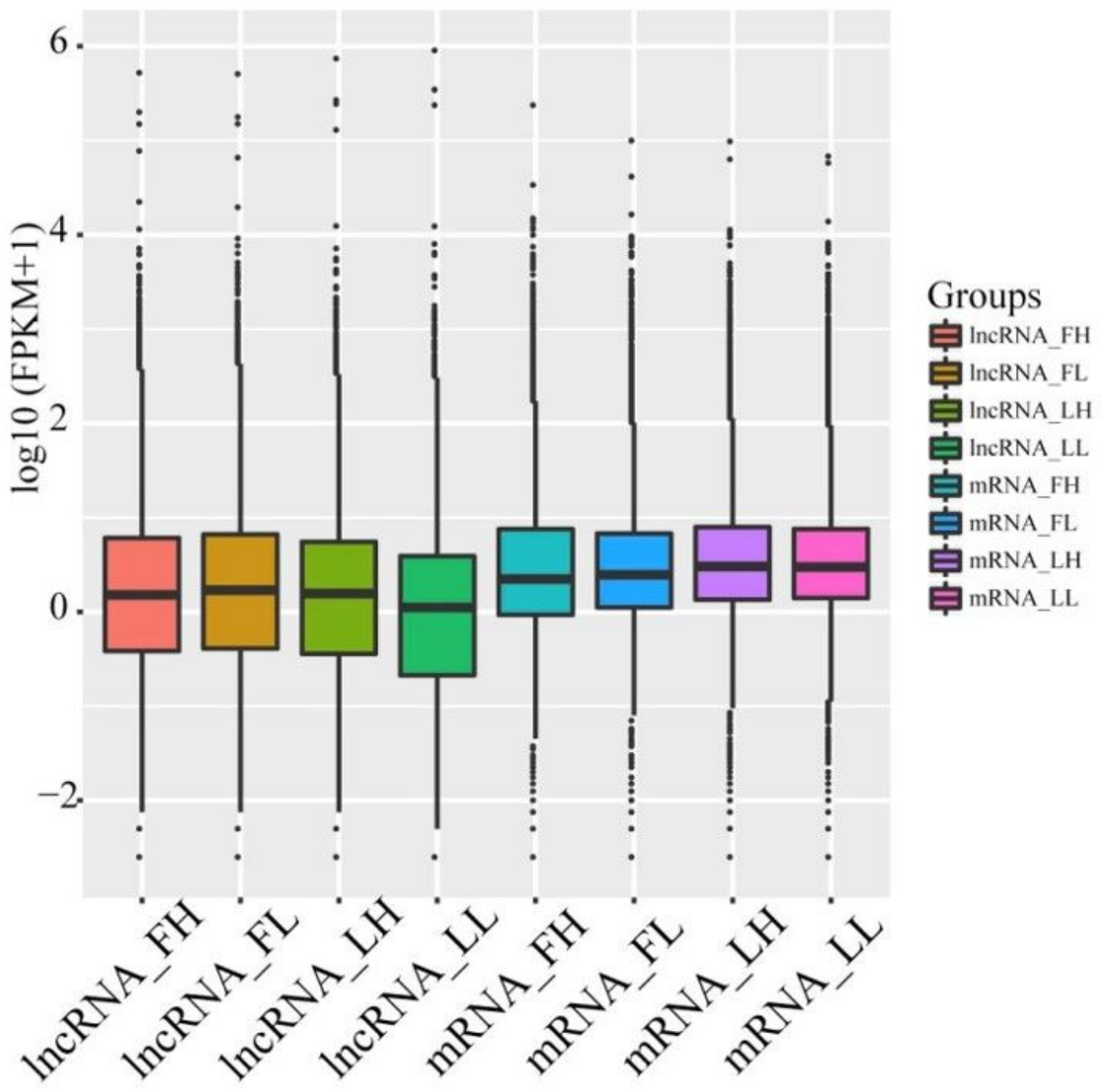


Figure 3

Expression levels of IncRNAs and mRNAs in four groups (LH, LL, FH and FL).

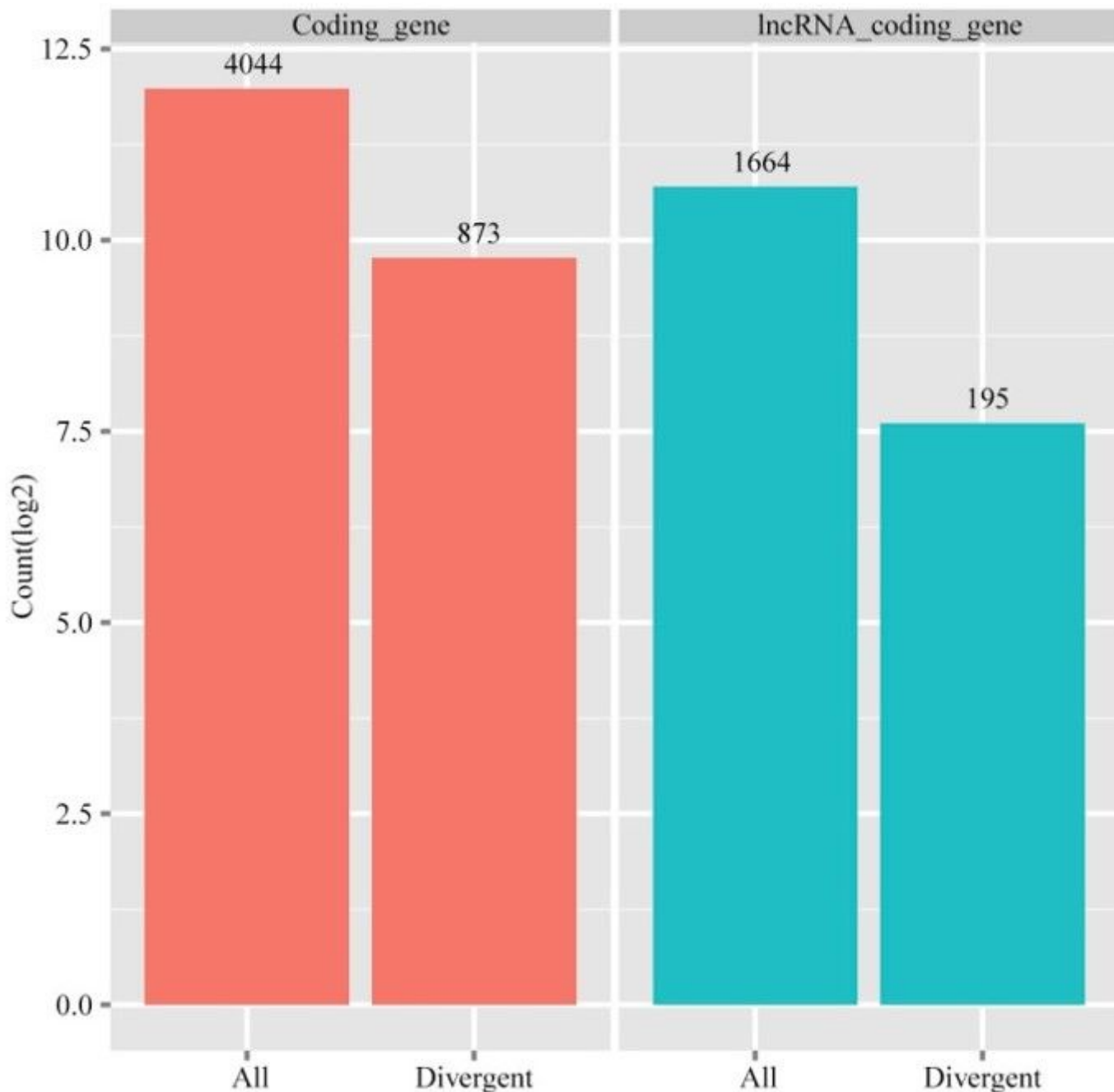


Figure 4

Number of gene pairs formed by lncRNAs and their neighboring coding genes. Proportion of divergent and all directions in coding gene pairs (red) and lncRNA: coding gene pairs (blue).

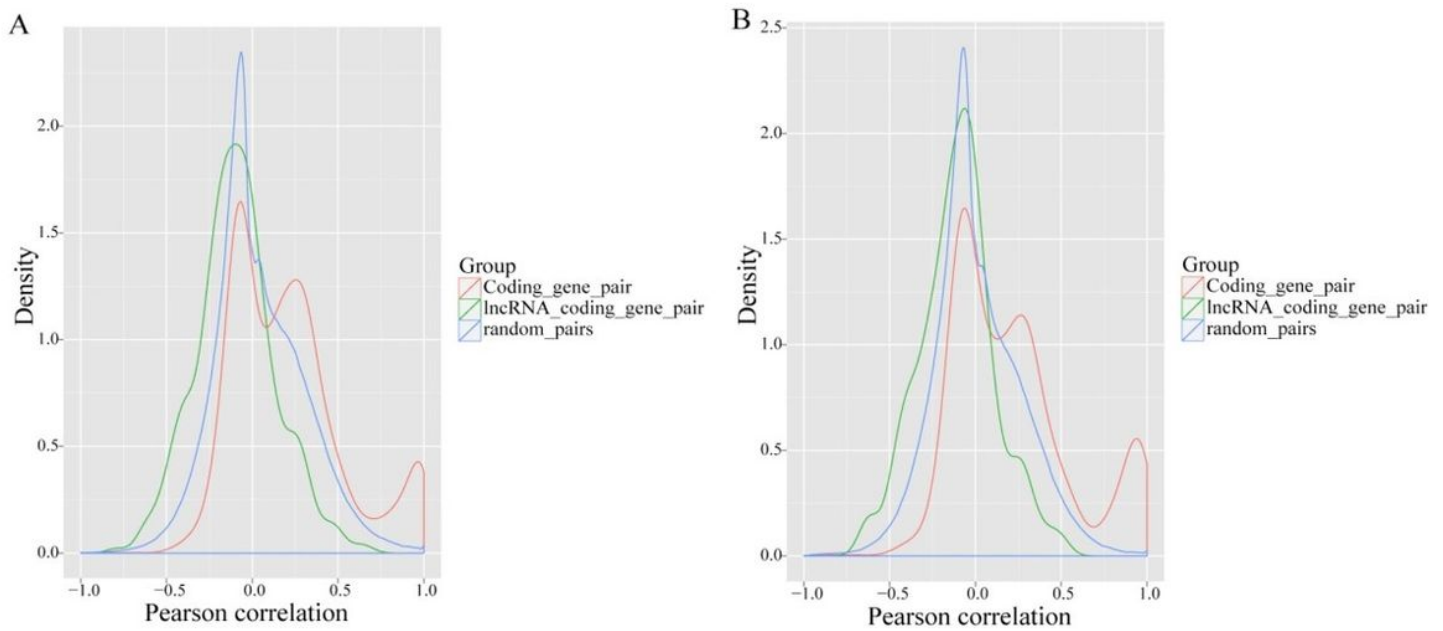


Figure 5

Correlation of expression patterns between pairs of neighboring genes. (A) distributions of Pearson correlation coefficients in expression levels between either 4,004 pairs of coding gene neighbors (red), 1,664 pairs of lncRNAs and their neighboring coding genes (green), or random pairs of genes (blue). (B) Distribution of Pearson correlation coefficients calculated as in A, but only for 195 pairs of divergently transcribed pairs of lncRNAs and protein-coding genes (green) or 873 pairs of divergently transcribed protein-coding genes (red).

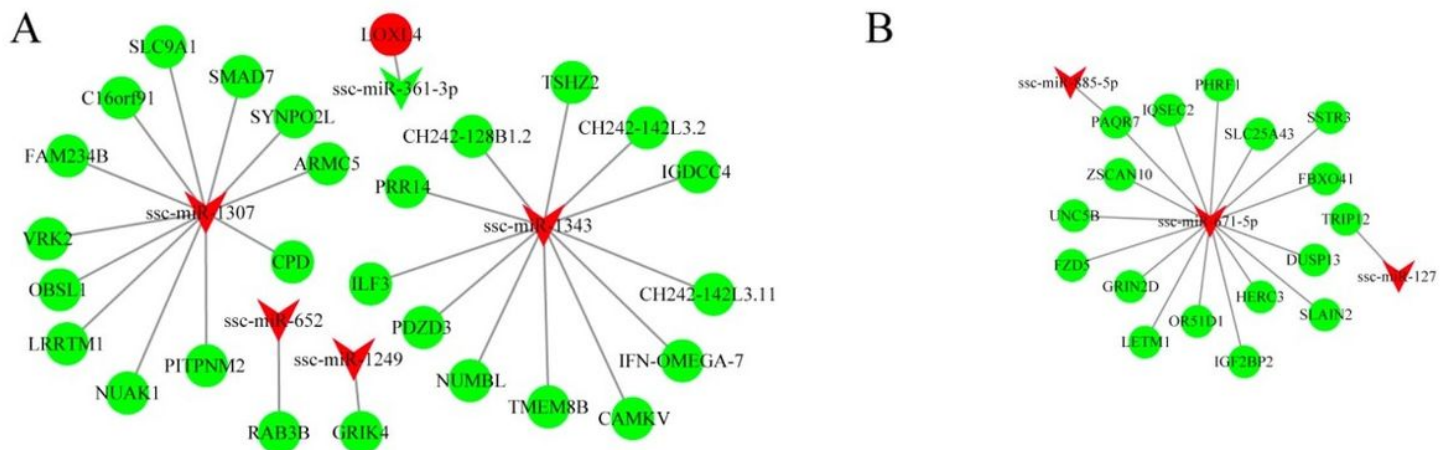
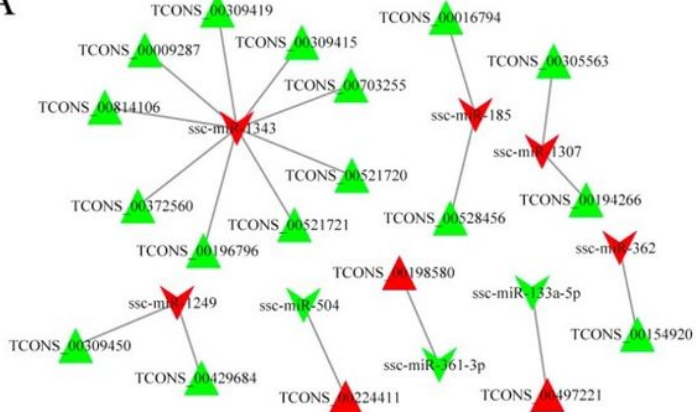
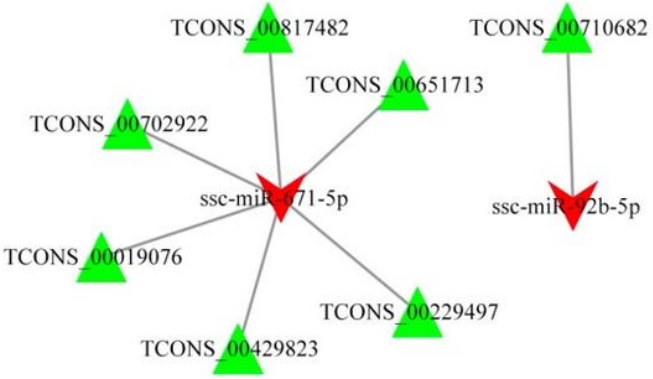
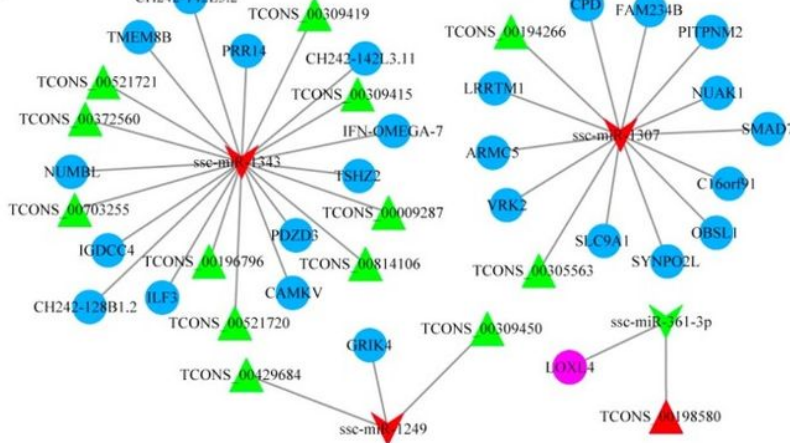
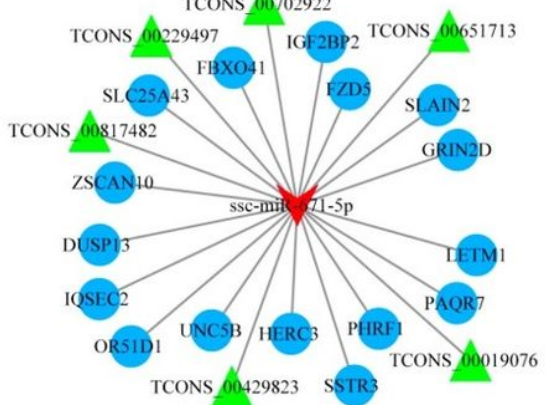


Figure 6

miRNA–mRNAs interaction network constructed and visualized. VEE and circular nodes represent miRNAs and mRNAs, respectively. Red nodes represent up-regulation, while green nodes represent down-regulation. (A) Interaction networks for comparison of LH vs. LL; (B) Interaction networks for comparison of FH vs. FL.

A**B****Figure 7**

Interaction networks of differentially expressed lncRNAs and miRNAs in ovarian tissue. Triangular nodes denote lncRNAs and VEE nodes denote miRNAs. Red nodes represent up-regulation and green nodes represent down-regulation. (A) Interaction networks for comparison of LH vs. LL. (B) Interaction networks for comparison of FH vs. FL.

A**B****Figure 8**

lncRNA–miRNA–mRNAs interaction network constructed and visualized. Red triangle nodes represent up-regulated lncRNAs, and green nodes represent down-regulated lncRNAs. Red VEE nodes indicate up-regulated miRNAs, and green nodes indicate down-regulated miRNAs. Purple circular nodes represent up-regulated mRNAs, and blue represent down-regulated mRNAs. (A) Interaction networks for comparison of LH vs. LL; (B) Interaction networks for comparison of FH vs. FL.

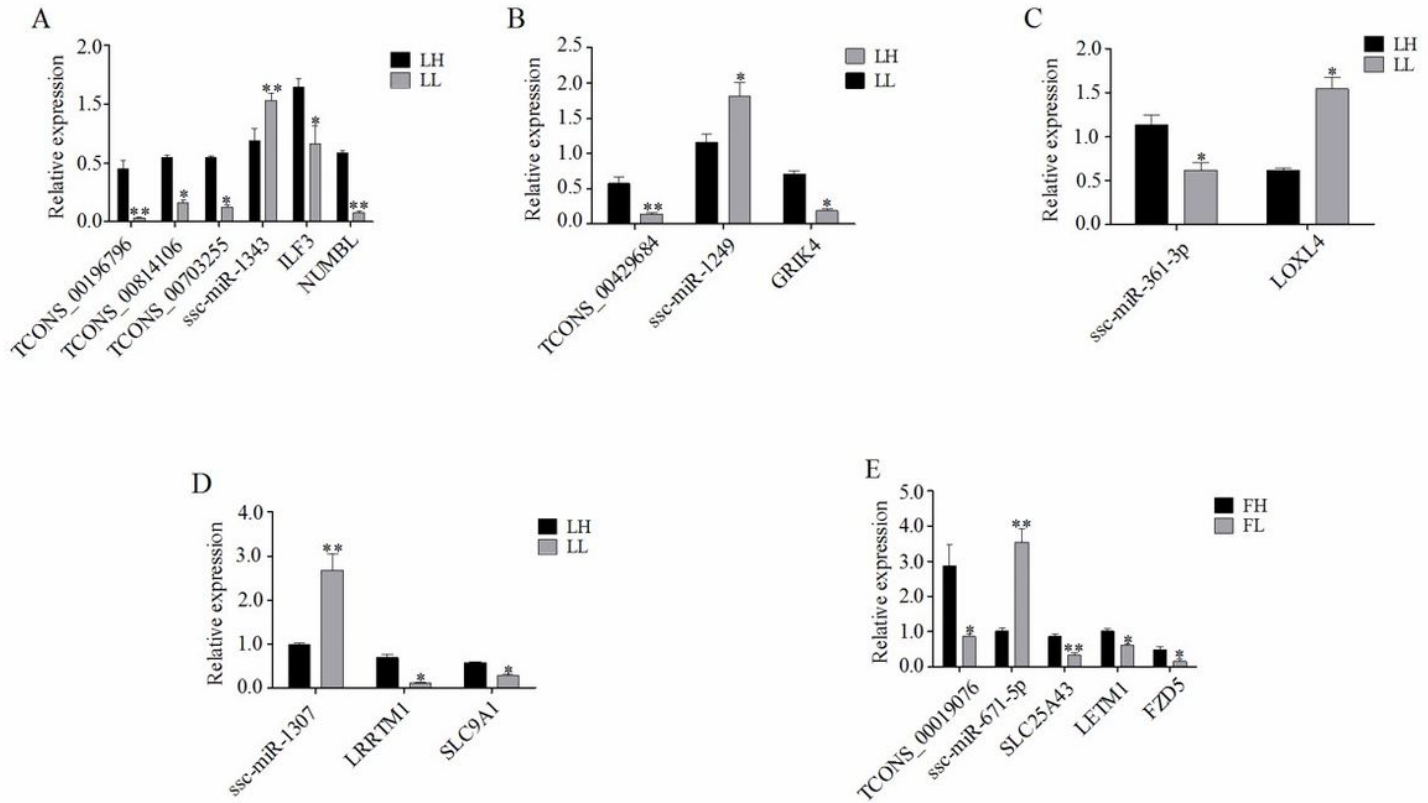


Figure 9

Expression levels of key genes by RT-qPCR. (A-D) LH vs. LL. (E) FH vs. FL. Data are presented as the mean \pm SD of three experiments. The data statistical significance was assessed by Student's t-tests. *P \leq 0.05, **P \leq 0.01 (Compared with the high fertility).

Supplementary Files

This is a list of supplementary files associated with this preprint. Click to download.

- Additionalfile5.xlsx
- Additionalfile8.xlsx
- Additionalfile7.xlsx
- Additionalfile1.xlsx
- Additionalfile9.xlsx
- Additionalfile4.xls
- Additionalfile6.xlsx
- Additionalfile3.xls
- Additionalfile10.xlsx
- Additionalfile2.xlsx